ORIGINAL RESEARCH ARTICLE

Radiometric and geomagnetic study of Kargi area, Marsabit – Kenya; radiation as possible cancer cause

Willis Aguko[1], Robert Kinyua[1], John Gitonga Githiri [1]

[1]Department of Physics, Jomo Kenyatta University of Agriculture and Technology, Nairobi, Kenya.

Corresponding author email: ***agukow8@gmail.com***

ABSTRACT

Radiometric and Magnetic studies were carried out in Kargi, at 2°28´36.9984˝ and 2°31´14.9988˝ N and 37°32´34.0008˝ and 37°36´6.9984˝ E. The focus of this study was to characterize radio-activity in soil and water, to find out possible causes of radiation in this area by studying magnetic intensities, zones considered anomalous with deepness to magnetic sources and outlining sub-surface structures. 117 soil and 14 water samples were picked from the entire Kargi and analyzed for radionuclides due to ^{40}K, ^{232}Th and ^{226}Ra. Measurement methods of proton magnetometer and γ-spectrometer using a high purity detector – germanium (HPGe) were basically utilized to gauge the magnetic survey and radiological hazard of radio-activities respectively. A total of 51 magnetic field measurements were taken on the eastern part of Kargi, a place suspected to have more concentration of radionuclides. The data was corrected and magnetic anomaly map plotted. Surfer 10 and Geosoft^{R} Oasis Montaj software were used to process the magnetic data. ^{40}K, ^{232}Th and ^{226}Ra had computed mean activities of 353.20±110.07, 7.97±3.98 and 7.38±2.59 Bq/kg for soil and 3.55±3.04, 2.20±2.74 and 52.68±25.07 Bql^{-1} for water respectively. Qualitative interpretation from magnetic intensity map showed lows and highs with variation in amplitude between-791 nT to 420 nT, an indication of lineament structures. Euler Deconvolution of magnetic data revealed the structures orientation, their depths together with the alignment of the anomalous zones to the base. Radially averaged power spectrum of magnetic data show depth estimates ranging between 100 m to 480 m indicating the total depth estimate to that that produced the observed anomalies. The values of annual effective doses together with Radium equivalent (Ra_{eq}) values for tested soil and water samples were below international standards making this area regarded safe to humans for agricultural practices, buildings, drinking and other purposes. Magnetic anomaly results show that radiation in the area could be originating from base rocks and not buried objects as the rock spreads along the area.

Keywords: Kargi, magnetic survey, radiometric, power spectrum

1.0 Introduction

Activity concentration from soil is considered a major determinant of natural back-ground radiation. Disintegration of rocks via natural and man-made processes help radionuclides to be eroded (Okpoli and Akingboye, 2016). Concentrations of natural radioactivity mainly depend on geological together with geographical states appearing at divergent degrees in soils of dissimilar

ISSN 1561-7645 (online)
doi: 10.4314/jagst.v24i2.4

geological regions. For out-door occupation gauging gamma dose-rate from terrestrial, approximation of natural radio-activity degree is key for geological samples, habitually ascertained from ^{40}K, ^{232}Th together with ^{226}Ra contentment (UNSCEAR, 2000).

Human beings and animals are un-protected by food-chain pollution happening as outcome of deposits of radio-nuclides to plant leaves, roots up-take from polluted soil, water and/or sediment (Aregunjo *et al.*, 2004) and also from straight consumption of contaminated waters (Avwiri and Agbalagba, 2007).

Researcher Otton, 1994 gives an explanation that between lower and moderate radiation doses, exposure to radiation both in human with animal may upsurge to long-term cancer disease manifestation and that the rate of genetic abnormal formations may surge by exposing to radiation. It is of importance to discover existing quantity of radio-activity in soil and drinking water for all area of residence to help cushion against its effects considered harmful (WHO, 2006). Physicians together with other professionals in health sector, as well as manufacturing workers, universities and nuclear power facilities are categories that might be exposed to ionizing radiation (Wafula *et al.,* 2022).

To comprehend the area's subsurface geology for detailed mapping, magnetic method (ground based) is used. This technique has extensively been employed in basement mapping (Folami, 1992). The technique needs measurement of magnetic components amplitude at distinct points through traverses mostly dispensed throughout the interest area of survey. Three components are measured in ground magnetic study, and include horizontal, vertical together with total components. The vertical components are largely applied in old studies to outline fractures, faults, deepness to magnetic vault together with other formations (Nettleton, 1976).

The aim of this work is to find out possible causes of radiation in this area by studying magnetic potencies, depicting sub-surface formations, anomalous zones with deepness to sources of magnetic and to meter radiological health hazard along with environmental radioactivity

ISSN 1561-7645 (online)
doi: 10.4314/jagst.v24i2.4

1.1 Study area

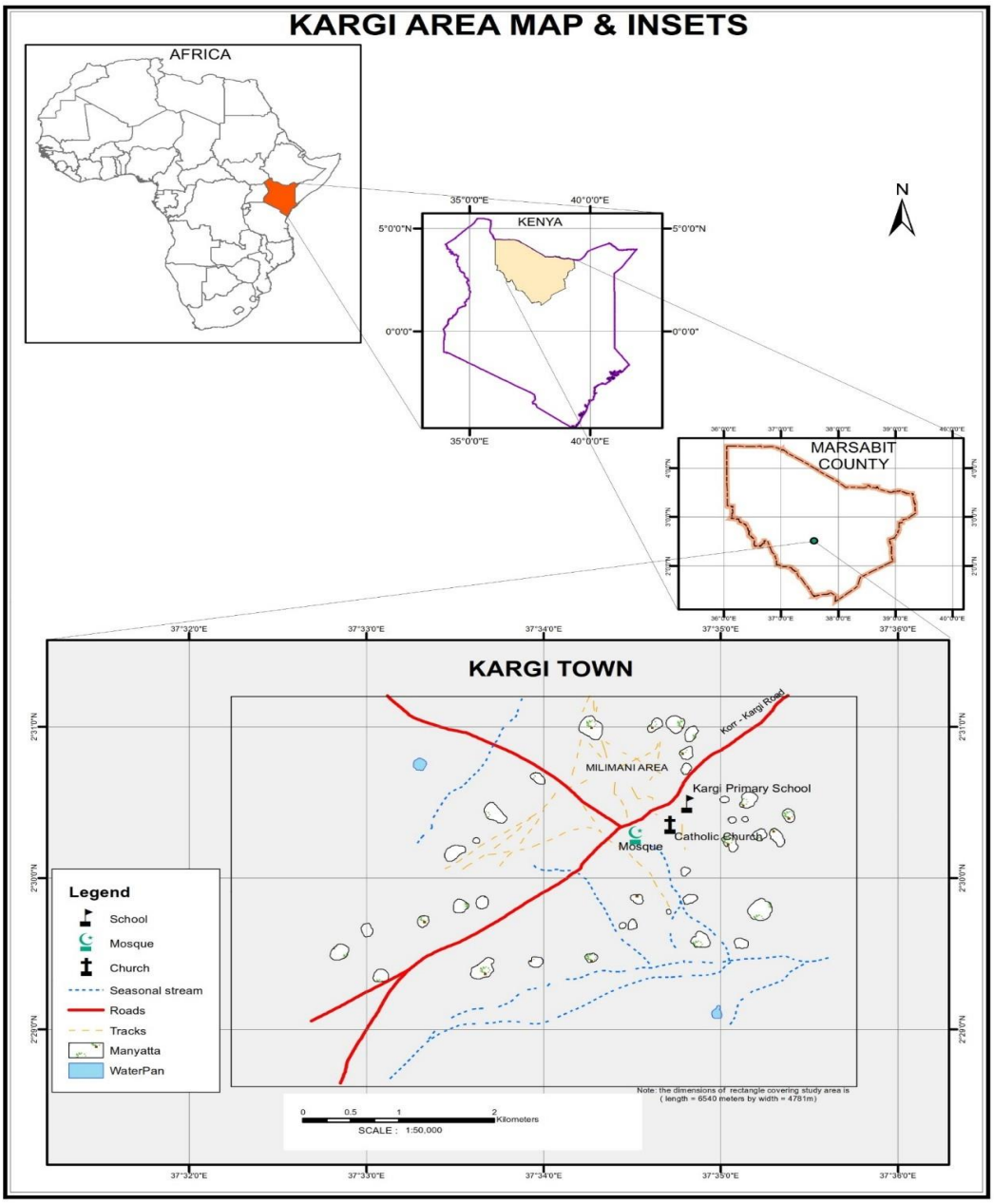

Figure 1. Study area (Aguko et al., 2020)

Figure 1 above shows the studied area. Kargi, approximately 70 km west of Marsabit town is in Marsabit County. Kargi borders chalbi, Gabra and Samburu. The area under study, located between 2°28′37′′ N and 2°31′15′′ N & 37°32′34′′E and 37°36′07′′ E is approximately 6.5 km by 4.8 km.

ISSN 1561-7645 (online)
doi: 10.4314/jagst.v24i2.4

1.2 Geology of Kargi.

Geology of study area is contained in sheet 20, a remote 12200 km^2 tract of the northern Kenya which was geologically mapped and geochemically surveyed at a reconnaissance scale in late 1984 by use of helicopter support. The sheet is bounded by both latitudes and longitudes 2° N and 3° N and 37° E and 38° E respectively (Report 108 (Reconnaissance) (1987)) as seen from figure 2.

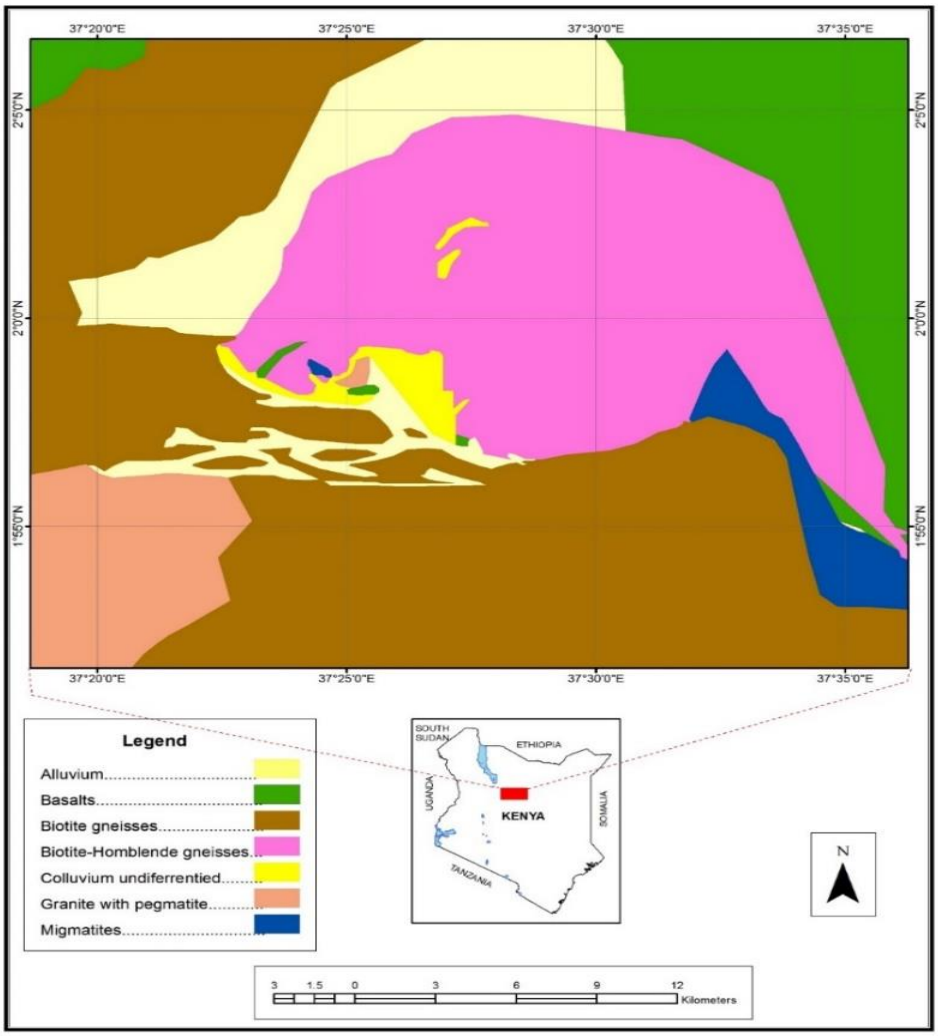

Figure 2: Rock types of Kargi.

From the report, Kargi is covered by Basalt capped mesas rocks which never rise more than 50 m above the adjacent plain and consists of a thin (less than 20 m) basalt cap invariably overlying sedimentary rock. A monotonous soil, rich in sand mantles the flat floor of the desert. However, there are subdued sand mounds suggesting that the area may formerly have been part of ample dune field. (Report 108 (Reconnaissance) (1987)).

Algas Basalt on western margin of the Marsabit lava, near Kargi dates to 2.5 ± 0.3 Ma. Basalt rocks contain plagioclase feldspar which is rich in radioactive minerals. Plagioclase feldspar is a

ISSN 1561-7645 (online)
doi: 10.4314/jagst.v24i2.4

member of feldspar group originating from igneous rocks (Report 108 (Reconnaissance) (1987)). Feldspar is from granite rocks, which are considered rich in minerals. Two main groups of feldspar are Potassium feldspar ("K-spar") and plagioclase ("plag"). Potassium (Potassic feldspar), Uranium (Uraninite, Urathorite, etc) and Thorium (Monazite, Zircon, etc) bearing minerals are traced to this rock type.

2.0 Sampling, materials and measurements

117 and 14 soil and water samples respectively were collected from Kargi, with 51 magnetic measurements done on the eastern side of study area, a place suspected to have more radionuclides. (IAEA TECDOC 486, 2019). EPA (1995), narrates factors determining the distances between sampling points in grid as the sampled area together with number of samples. For soil sampling, systematic grid-sampling, contemplated impartial sampling method was exercised. By dividing the area in to regular squares each of about 500.0 m x 500.0 m, the area was marked to aid get a better sampling representation. Soil samples were collected from the nodes (Figure 2). To avoid soil samples pollution from surface with leaves along with other contaminants, samples were picked approximately 10 centimeters from the soil surface (Monika *et al*., 2010). Kargi water sources are categorized as boreholes (shallow wells), Tap/Water kiosks and dams/wells. Water samples were drawn from these sources in standard polyethylene (0.5-litre) plastic containers, packaged, well-marked and laboratory transported. The plastic containers were washed clean before respective rinsing with weak hydrochloric acid and distilled water before filling with collected water-samples. Addition of 0.25-ml strong Nitric acid (HNO_3) to collected water samples, helping prevent any loss of radium isotopes throughout the walls of the plastic container along with avoiding growth of micro-organisms (Hany and Abdallah, 2014). The containers were bream-filled and tightly closed to prevent air enter the container.

All the collected water samples were clearly marked, laboratory transported for further preparation and analysis. Figures 3 and 4 give soil samples and magnetic reading plans while Table 1 shows sources of water samples collection, activity concentrations and Radium equivalent values and their locations in the map. Again, figure 4 shows magnetic anomaly for the area.

ISSN 1561-7645 (online)
doi: 10.4314/jagst.v24i2.4

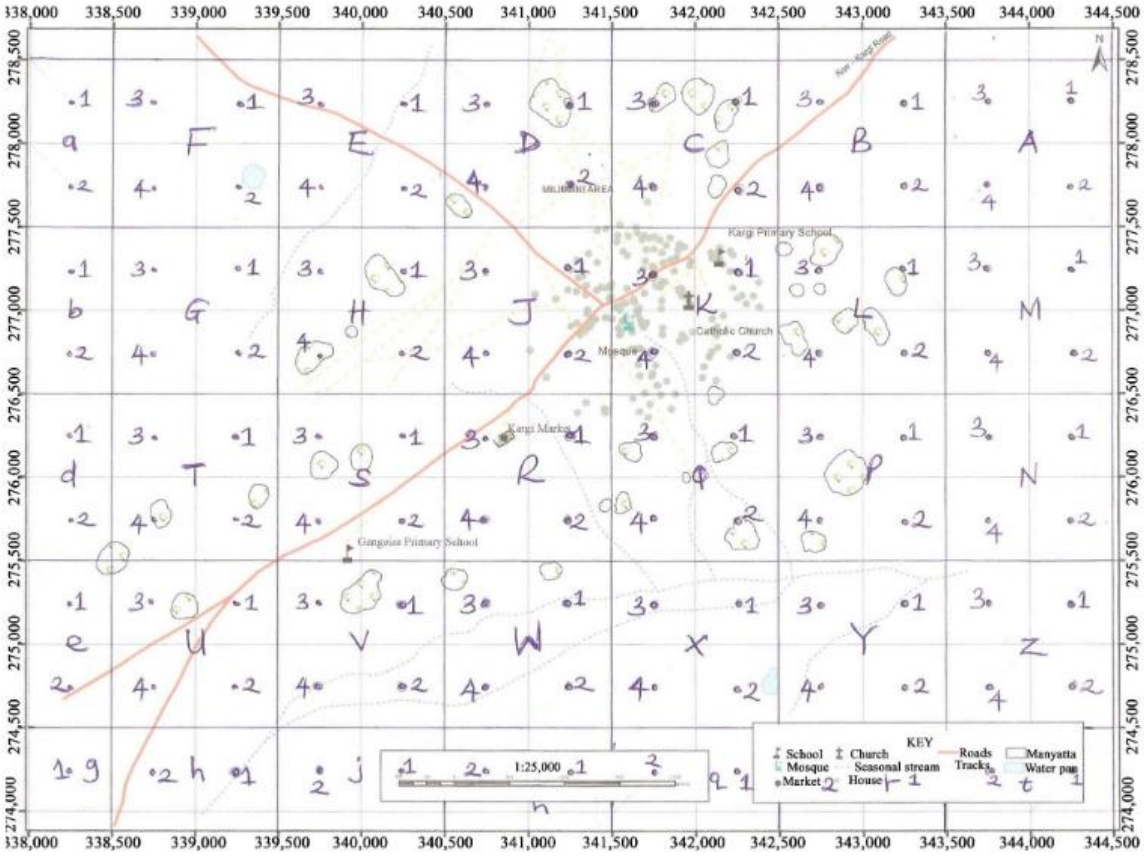

Figure 3: Soil sample collection plan for Kargi (Aguko et al., 2020)

ISSN 1561-7645 (online)
doi: 10.4314/jagst.v24i2.4

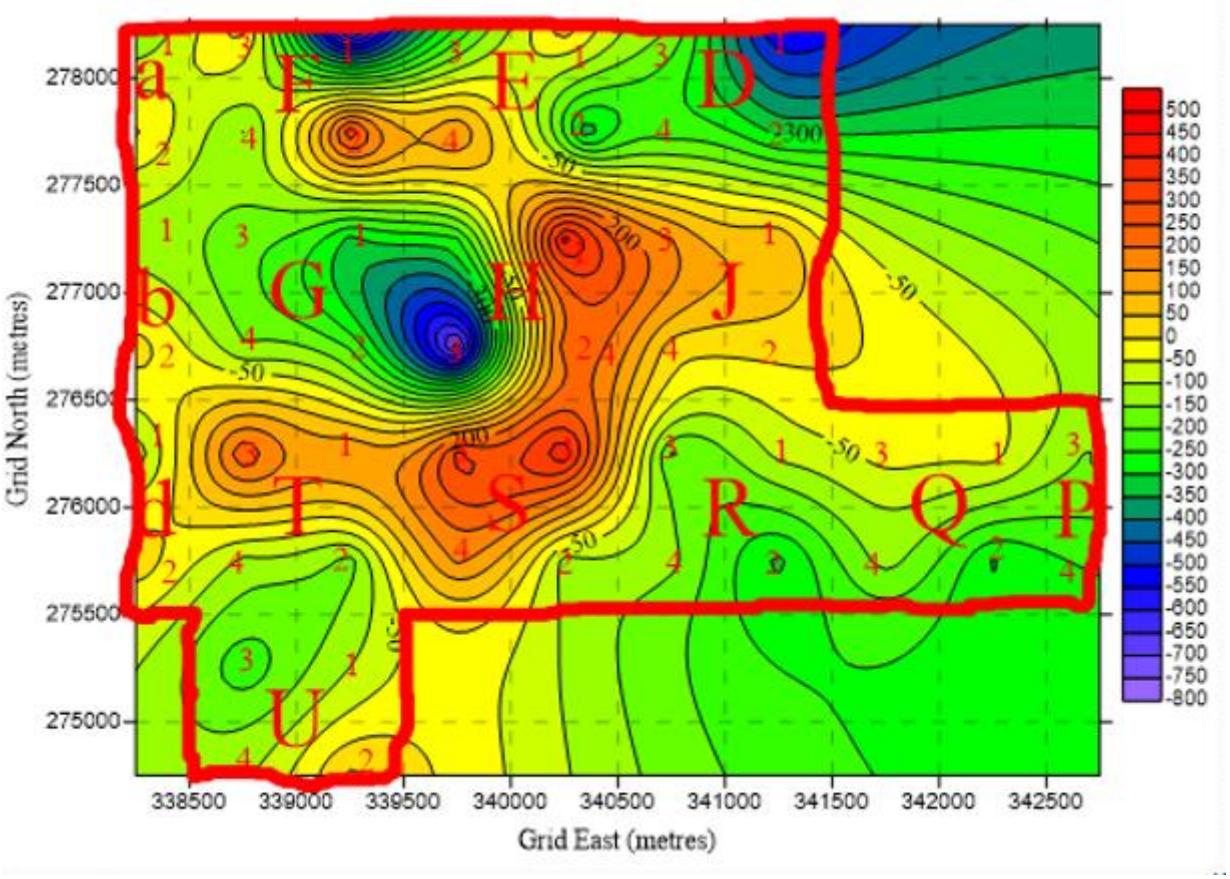

Figure 4: Plotted Magnetic anomaly map for Kargi

Table 1: Water sample identity, Water source, mean activity concentration (Bq/l) along with equivalent Radium (Bq/l).

Sample identity	WATER SOURCE		Mean activity Concentration, Bql^{-1}			Ra_{eq}, $Bqkg^{-1}$
	(Longitude) Easting, E	(Latitude) Northing, N	^{226}Ra	^{232}Th	^{40}K	
W_1	37.591971	2.517675	3.63±2.79	0.12±2.12	71.33±10.81	9.29
W_2	37.596068	2.503742	4.55±1.81	2.64±2.14	54.63±8.67	12.53
W_3	37.583479	2.495335	7.84±5.05	1.71±6.03	36.01±28.50	13.06
W_4	37.58304	2.485123	2.08±2.19	0.98±3.16	68.92±9.92	8.79
W_5	37.549452	2.486624	3.39±4.39	7.99±4.61	57.72±24.74	19.26
W_6	37.553105	2.492507	6.04±2.18	3.94±3.76	77.16±14.58	17.62
W_7	37.568392	2.509391	5.66±2.40	-2.00±2.37	45.68±19.38	6.32
W_8	37.56921	2.501813	6.41±2.85	1.90±3.07	64.45±14.13	14.09
W_9	37.569227	2.501994	7.66±2.97	4.37±3.95	60.49±19.75	18.57
W_{10}	37.570479	2.492526	0.59±2.01	3.12±3.16	42.33±14.70	8.30
W_{11}	37.570588	2.499644	3.59±2.21	0.19±2.81	72.53±11.57	9.45
W_{12}	37.570606	2.499707	0.27±2.63	0.54±3.85	-2.36±13.22	0.84
W_{13}	37.576149	2.503919	-1.82±3.42	6.09±4.74	81.22±22.00	13.14
W_{14}	37.575952	2.503693	-0.25±2.70	-0.85±2.55	7.61±12.69	-0.88

ISSN 1561-7645 (online)
doi: 10.4314/jagst.v24i2.4

Table 2: Soil sample collection plan, mean activity concentration (Bq/l) and equivalent Radium (Bq/l).

Sample area code	Number of collected soil samples	Sampling area, km^{20}	Activity, Bq/kg ^{232}Th	^{238}U	^{40}K	Radium equivalent activity, (Ra_{eq}) in $Bqkg^{-1}$
A	4	1.00	4.32±2.04	5.80±1.92	276.14±46.70	33.24±3.40
B	4	1.00	5.63±1.86	6.78±2.25	405.39±84.53	46.04±5.52
C	4	1.00	7.03±2.29	6.08±1.23	324.42±70.37	41.11±4.75
D	4	1.00	8.42±2.23	6.83±1.59	287.93±76.28	41.04±8.04
E	4	1.00	10.07±4.31	6.75±3.02	281.74±119.85	42.84±14.55
F	4	1.00	9.35±5.51	8.86±1.60	361.70±117.59	50.08±18.37
G	4	1.00	8.96±3.21	7.77±1.44	455.26±101.45	55.64±7.39
H	4	1.00	6.97±3.65	7.89±1.30	259.89±54.69	37.86±6.61
J	4	1.00	8.43±0.33	6.30±1.82	242.56±89.52	37.03±7.61
K	4	1.00	6.84±1.12	9.75±5.62	287.13±98.99	41.64±13.41
L	4	1.00	6.62±2.61	5.93±0.70	436.01±40.84	48.96±6.08
M	4	1.00	6.37±0.68	5.71±1.16	330.39±21.92	40.25±1.65
N	4	1.00	9.70±5.47	6.13±0.68	308.68±116.39	43.76±16.76
P	4	1.00	2.74±2.59	6.07±2.40	349.51±70.58	36.91±2.73
Q	4	1.00	9.70±3.70	8.51±2.73	405.47±155.79	53.60±17.31
R	4	1.00	7.49±2.78	8.72±2.26	398.65±33.46	50.13±6.43
S	4	1.00	6.71±1.63	7.93±0.24	330.12±49.75	42.94±3.89
T	4	1.00	10.66±5.89	10.53±3.51	425.98±131.73	58.57±18.03
U	4	1.00	8.33±3.20	7.73±1.75	380.98±168.08	48.97±16.99
V	4	1.00	8.96±12.51	6.36±3.62	440.90±151.62	53.12±32.96
W	4	1.00	6.54±4.26	6.85±1.33	450.12±52.19	50.86±9.57
X	4	1.00	9.34±5.98	9.05±4.68	380.08±264.93	51.67±29.07
Y	4	1.00	9.31±5.13	11.96±2.81	231.27±86.67	43.07±11.16
Z	4	1.00	12.34±3.14	8.53±2.09	311.59±33.34	50.17±5.64
a	2	0.50	7.70±0.86	5.61±1.61	438.06±143.71	50.34±10.68
b	2	0.50	9.75±5.96	5.54±0.32	472.49±57.64	55.85±3.77
d	2	0.50	8.73±4.47	4.04±1.05	369.76±115.25	45.00±1.44
e	2	0.50	6.98±0.07	6.78±1.77	404.28±82.71	47.89±8.24
g	1	0.25	9.89±0.00	5.75±0.00	407.13±0.00	51.24±0.00
h	2	0.50	8.65±0.64	8.58±2.57	387.28±42.80	50.76±6.78
j	2	0.50	9.83±0.14	6.12±2.27	372.98±32.05	48.89±0.40
n	2	0.50	6.87±0.69	7.61±0.08	333.28±32.51	43.09±1.59
q	2	0.50	5.18±0.71	6.46±2.55	286.89±11.60	35.95±4.46
r	2	0.50	8.54±1.34	4.94±1.21	324.75±10.59	42.15±1.53
t	2	0.50	8.27±2.07	8.78±1.49	259.57±128.33	40.58±11.35

ISSN 1561-7645 (online)
doi: 10.4314/jagst.v24i2.4

3.0 Results and Discussion

For radiometric results, tables 1 and 2 for water and soil respectively give mean activity concentrations and radium equivalent values for Kargi. For water samples analyzed, ^{40}K, ^{238}U, ^{232}Th and Ra_{eq} values ranged from -2.36±13.22 to 81.22±22.00, -1.82±3.42 to 7.84±5.05, -2.00±2.37 to 7.99±4.61 and -0.88 to 19.26 Bql^{-1} respectively with average and standard deviation of 52.68±25.07, 3.55±3.04, 2.20±2.74 and 10.74±6.03 $Bqkg^{-1}$ respectively. Soil samples analysis yielded for ^{40}K, ^{238}U, ^{232}Th and Ra_{eq} values from 231.27±86.67 to 450.12±52.19, 4.04±1.05 to 11.96±2.81, 2.74±2.59 to 12.34±3.14 and 33.24±3.40 to 58.57±18.03 $Bqkg^{-1}$ respectively with average and standard deviation of 354.81±67.06, 7.23±1.67, 8.03±1.91 and 46.04±6.28 $Bqkg^{-1}$ respectively. Globally, recommended values for soil activities are respectively 37.0, 33.0, 400.0 Bq/kg (UNSCEAR, 2008) along with 370 $Bq{\cdot}kg^{-1}$ (Lu & Zhang, 2006), while for water are 10.0 Bql^{-1}, 1.0 Bql^{-1}, 10.0 Bql^{-1} respective (UNSCEAR, 2000 and WHO 2008 Standards) along with 370 $Bqkg^{-1}$ as guided by Organization for Economic Co-operation and Development, OECD and (Lu & Zang, 2006). Figures 5 and 6 summarizes activity concentrations for water and soil respectively.

Figure 5. ^{226}Ra, ^{232}Th and ^{40}K activity values of samples in investigated area – water samples.

ISSN 1561-7645 (online)
doi: 10.4314/jagst.v24i2.4

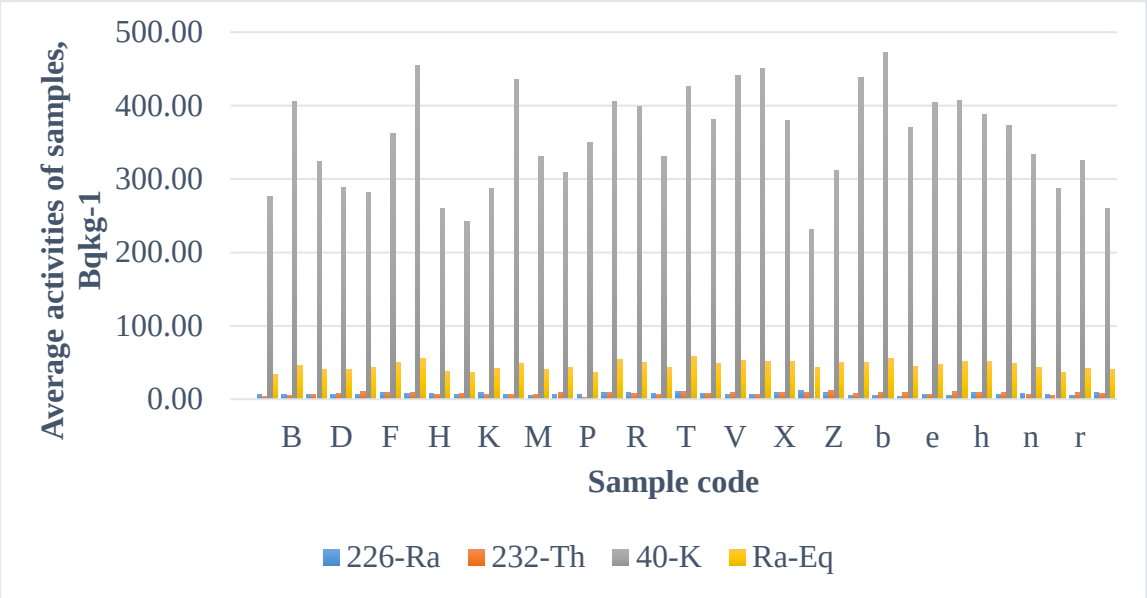

Figure 6. ^{226}Ra, ^{232}Th, ^{40}K together with Ra_{eq} activity values of samples in Kargi - Soil.

All calculated mean activities for ^{232}Th, ^{226}Ra, ^{40}K and Ra_{eq} from the soil were found less global values recommended. 23.87±3.48 nGy/h was the mean computed absorbed dose rates for all picked soil samples against 54 nGy/h – global median value (UNSCEAR, 2000). These values ranged between 16.05±1.10 and 29.34±1.32 nGy/h. For water results, the mean activities for Kargi was 5 times higher, low, 2 times higher and low against the worldwide accepted limit for ^{40}K, ^{226}Ra, ^{232}Th and Ra_{eq} respectively.

The AEDE (De) values as calculated from soil samples, were lower than world acceptable value of 1 mSv/y (ICRP, 2000) with an average and standard deviation of 0.14±0.02 mSv/y, ranging from 0.12±0.01 to 0.18±0.05 mSv/y. Excess life-time cancer risk, considered an added risk a person might have on developing cancer disease if receptive to extended period to cancer causing materials. By using 70-years as average life duration taking a risk factor of 0.05 per Sv (ICRP, 2007; Taskin *et al*., 2009) and average annual effective dose rate of 0.14 mSv/y, then excess cancer risk is found to be 0.05%. This value is less than global value of 0.145% (Taskin *et al.*, 2009; UNSCEAR, 2000).

Tzortzis & Tsertos (2004) and Al-Hamarneh & Awadalla (2009) pointed that a low or high value of Th/U, measured in some researched locations may be total indication of a reduction or addition in uranium or thorium respectively due to alteration of natural happenings in that particular area. They postulated the theoretical normal continental crust values of Th/U elemental ratios to 3.0. From the study, Th/U calculated results varied from 1.18±0.90 to 6.34±1.73 with average and standard deviation of 3.56±1.14. Other computed correlation of K/U along with K/Th varied from 0.83± 0.47 to 3.89±2.12 along with 0.33±0.10 to 1.95±2.41 with average and standard deviations of 2.15±0.68 and 0.67±0.29 respectively. Correlations

ISSN 1561-7645 (online)
doi: 10.4314/jagst.v24i2.4

existing between activities ^{232}Th and ^{238}U, ^{40}K and ^{238}U and ^{40}K and ^{232}Th displayed a weak relationship existing on ^{232}Th against ^{238}U, ^{40}K against ^{232}Th along with ^{40}K against ^{238}U with correlation coefficients of 0.404, 0.320 and 0.133 respective.

3.1 Magnetic maps

The obtained magnetic data along traverses at the eastern side of Kargi was used in producing Total magnetic intensity (TMI) map to help deduce the magnetic potency range of the rocks with geologic structures and areas that are susceptible. An amplitude range between -791.4 nT and 419.9 nT for the Total magnetic intensity map was seen. These values are not uncommon in a vault complex (Telford *et al.,* 1990). Due to the mineral content in the surface and sub-surface rocks and its structural mapping, the total magnetic potency ranges from one location to another. Figure 7 shows the Total magnetic intensity (TMI) maps for studied area. Areas denoted by A, B and C are areas considered to have high amplitude of magnetic intensity; suggesting the presence of the vault rocks transpiring at shallow deepness down the surface. Areas with the low negative amplitude in magnetic intensity marked D is an area indicating the zones of weaknesses that suggest the presence of geologic structures like fractures, faults and lineaments.

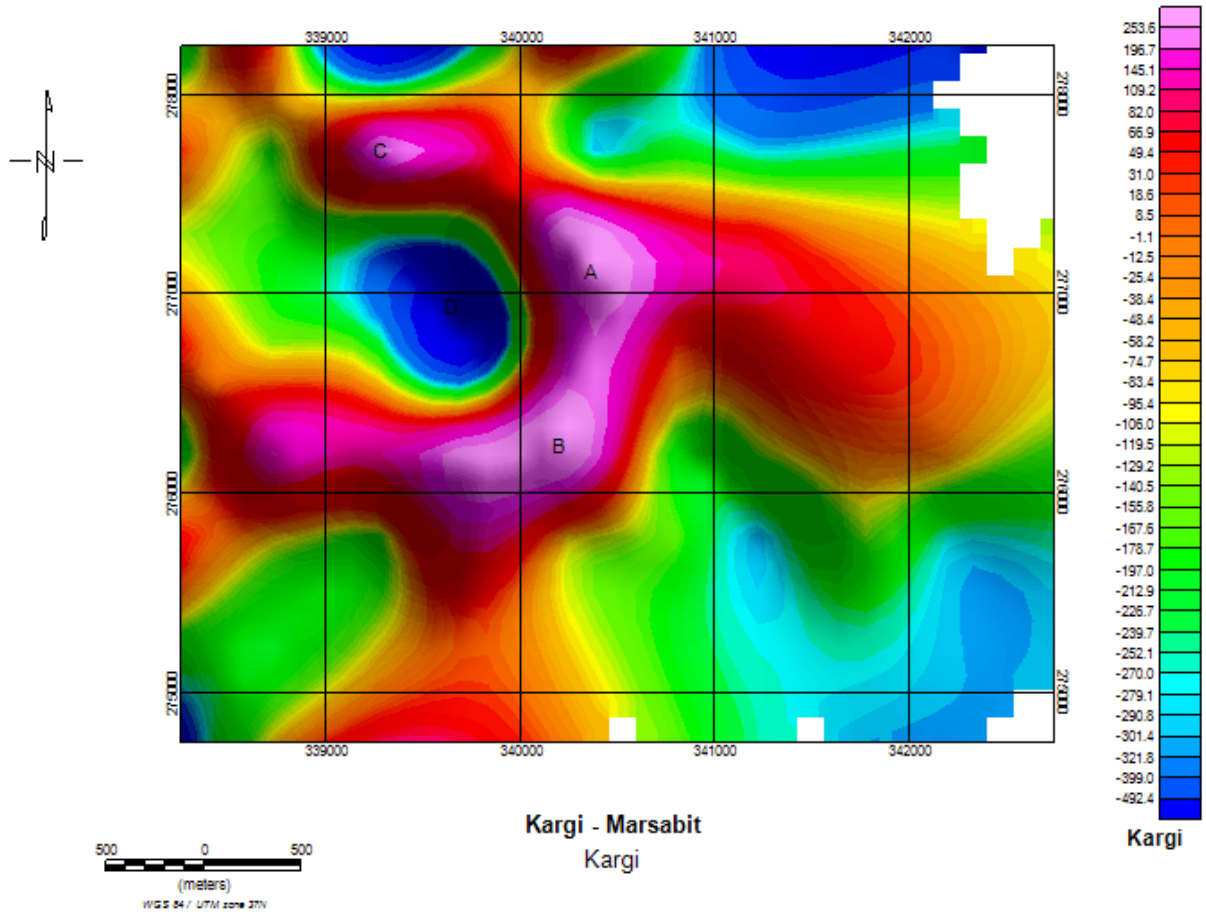

Figure 7: Total magnetic intensity (TMI) map of Kargi area.

ISSN 1561-7645 (online)
doi: 10.4314/jagst.v24i2.4

The ranging magnetic potency suggests ranging magnetic materials correlated with the rock types in the area. According to Gunn *et al.,* 1997a, the amplitude of a magnetic anomaly is directly proportional to magnetization and depends on magnetic susceptibility of the rocks.

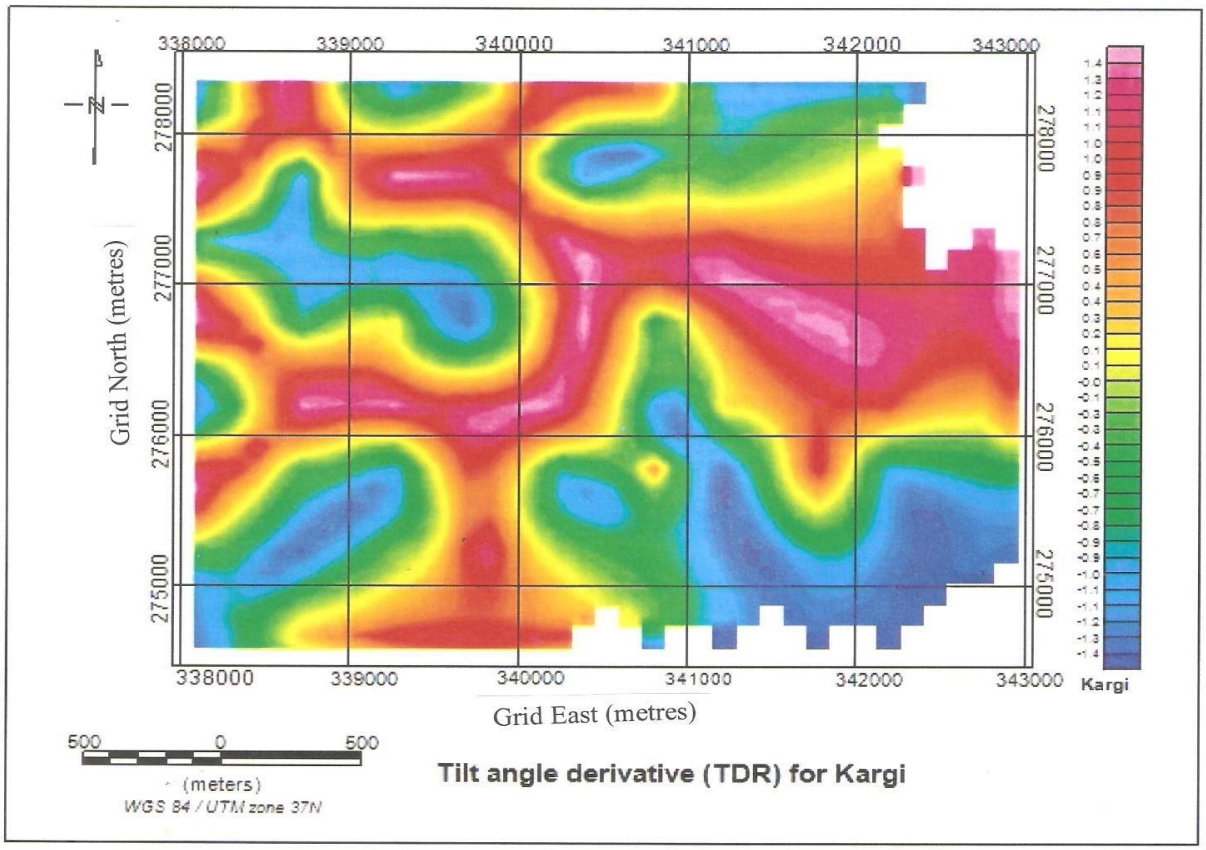

Figure 8: Tilt angle derivative (TDR) derived from TMI of the Study Area.

The Tilt Derivative (TDR) together with its Horizontal component (HD_TDR) maps for area under study were derived from the tilt derivative filter applied to the TMI grids to establish fault & folds, the contacts & edges or boundaries of magnetic sources as in figures 8 and 9, and to intensify both frail and sturdy magnetic anomalies of the area placing an anomaly directly on top of its source. Tilt angle derivative (TDR) of TMI establishes the edges of structures and especially at shallow deepness using a theory that zero-contours are the edges of the structure (Salem *et al.,* 2007). It is observed that the zero contours gauge the location of instantaneous changes in magnetic susceptibility values. The zero contour lines are represented by yellow colour, areas showing lineaments are those with blue colour, while those with colour red are the un-deformed or un-weathered basement. Figure 8 shows the resolution of the tilt angle derivative (TDR) in the vertical direction while figure 9 shows the resolution of the tilt angle derivative (TDR) in the horizontal direction of the study area. Comparing Figure 8 and Figure 9 below, the TDR image shows different lineaments and contacts in the area.

ISSN 1561-7645 (online)
doi: 10.4314/jagst.v24i2.4

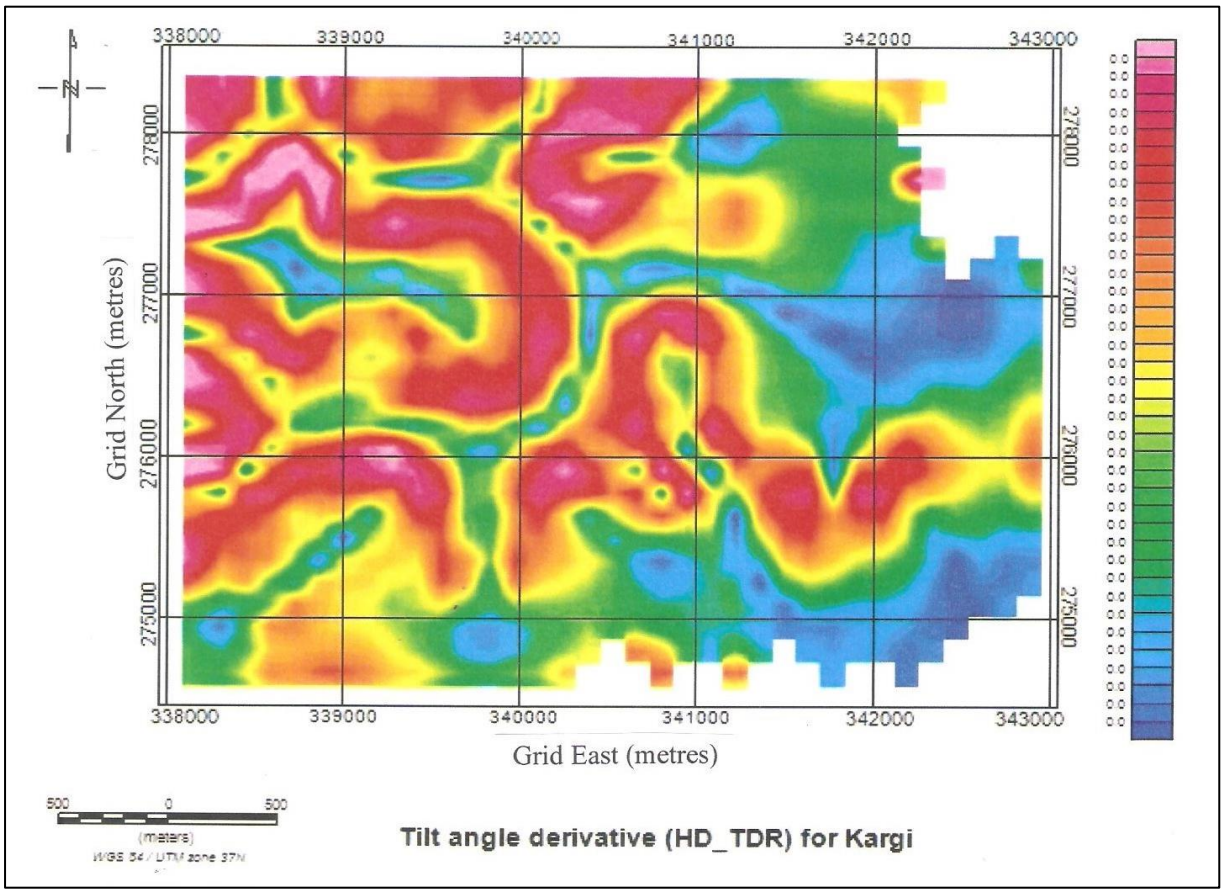

Figure 9: Tilt angle derivative (HD_TDR) in the horizontal direction derived from TMI of the Study Area.

Figure 10 shows the Radial Average Power Spectrum (RAPS) of the study area with the total depth estimate to the top of geologic sources that occasioned the observed anomalies in the magnetic map and were ascertained using spectral analysis. For the study area, the depths to the magnetic sources ranges from 100 m to 480 m. The deepness of the anomalous bodies in in the area showed that the anomalous bodies are very close to the surface because the depth estimations from the power spectrum is indicating near surface of the bodies.

ISSN 1561-7645 (online)
doi: 10.4314/jagst.v24i2.4

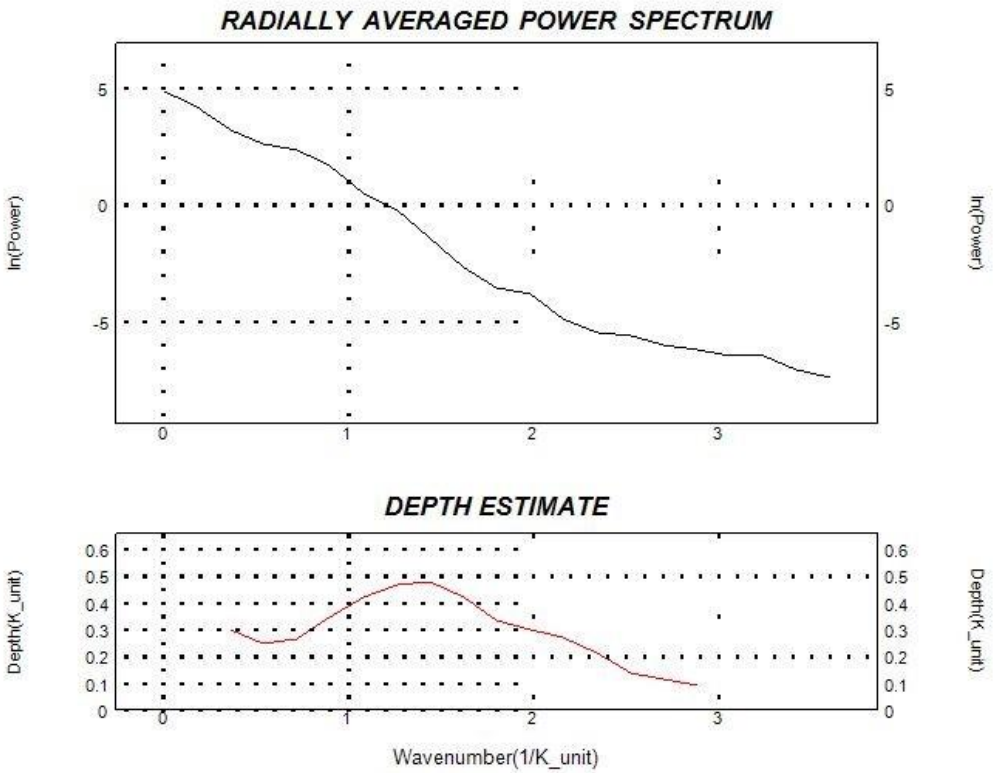

Figure 10: Radially Averaged Power Spectrum (RAPS) and Deepness Estimate

4.0 Conclusion

The study has shown the importance and worthiness of radiometric and magnetics methods in effective mapping out of lithologies, characterizing magnetic intensities and radionuclides, delineating subsurface structures, anomalous magnetic sources. Inspection of the individual Total (TMI) maps revealed the range of the magnetic intensity of the rocks with the infilled geologic materials, geologic structures and areas that are susceptible of intensity with amplitude variation between-791.4 nT and 419.9 nT. The derivative (TDR) with the horizontal component (HD_TDR) showed that the lineament structures to be trending approximately in dipping, vertical and horizontal directions with break in subtle as seen from the shape of the structures. It is evident that the TMI map has similar trends of NE-SW, NW-SE and some perpendicular to the strike direction with those on the TDR and HD_TDR maps. The varying magnetic potency suggests varying magnetic materials linked with the rock types in the area. The radiometric profiles established evidences from the geologic formations about the radiation levels of the under investigation. Geologic events like intensive weathering of the feldspar-bearing-minerals in parent rocks into clay particles have been eroded from their source and low enrichment of the parent rocks in potassic feldspar in relation to other feldspar minerals must have caused the radioactivity level K, U and Th in area. Gamma rays among the other radiations have the highest energy and will perforate several hundred feet in the atmosphere but a few inches of earth attenuate them. Radiation elements must occur in outcrop or sediments to be detected. The concentration and spatial distribution of radioactive elements such as uranium,

ISSN 1561-7645 (online)
doi: 10.4314/jagst.v24i2.4

thorium and potassium from the upper 10-60 cm layer of earth's surface non vegetative may be measured in radiometric surveys (Gandhi and Sarkar, 2016).

The elevated radiation level of ^{40}K in some parts of the western side of Kargi as evidenced from table 2, with some ^{238}U and ^{232}Th, suggests that the geologic formation of the area is richer in potassium-bearing minerals, Uranium-bearing-minerals and Thorium bearing-minerals respectively. Weathering rate of the parent rocks, terrestrial gamma radiation enrichment in parent rocks, and low fracturing density system of the parent rocks that would have accumulated materials that are non-radioactive could all have accounted for the radioactivity level of the area. Because Th/U calculated value was greater than the recommended, it can be concluded from the study that there could have been a fractionation during weathering period or metasomatic activity of the radioelements involvement. This study also reveals that the mining activities in the nearby study area could have affected the geologic formation causing more fracturing in rocks and pronounced subsurface structures as a result of mining that could have served as passage for leachates from pollutants as well as the level of radiation in the study area.

Nevertheless, the study found that results from analyzed soil and water samples from the study area when compared with international standard show that the area is safe to humans for agricultural practices, drinking, mining and domestic purposes.

5.0 Acknowledgements

5.1 Funding

None

5.2 General acknowledgement

Great indebtedness is extended to the following institutions for their invaluable support: Kenya Bureau of Standards (KEBS) for equipment and assistance in sample preparation, National Oil Corporation of Kenya for geomagnetic maps support, Jomo Kenyatta University of Agriculture and Technology (JKUAT) for the use of the grinder and Institute of Nuclear Science, University of Nairobi for the use of the Hyper-germanium detector.

5.3 Conflict of interest

None.

5.4 Ethical considerations

None

6.0 References

Aguko, W., Kinyua, R. and Githiri, J. (2020) Natural Radioactivity and Excess Lifetime Cancer Risk Associated with Soil in Kargi Area, Marsabit-Kenya. *Journal of Geoscience and Environment Protection*, **8**, 127-143. doi: 10.4236/gep.2020.812008.

Al-Hamarne, I. F., & Awadallah, M. I. (2009). Soil Radioactivity Levels and Radiation Hazard Assessment in the Highlands of Northern JORDAN. Radiation Measurements, 44, 102-110. https://doi.org/10.1016/j.radmeas.2008.11.005

Aregunjo, A. M., Farai, I. P., & Fuwape, I. A. (2004). Impact of oil and gas industry on the natural radioactivity distribution in the Delta region of Nigeria. Nigeria Journal of Physics 16 (131), 136.

Avwiri, G. O., & Agbalagba, E. O. (2007). Survey of gross alpha and gross beta radionuclide activity in Okpare–Creek, Delta State, Nigeria. Asian Journal of Applied Science, 7 (22), 3542–3546.

EPA (1995). Representative Sampling Guidance, Vol. 4: Soil, EPA/540/R-95/141, EPA, Washington, DC.

Folami S.L. 1992. Interpretation of Aero magnetic Anomalies in Iwaraja area, Southwestern Nigeria. Journal of Mining and Geology, 28(2), 391–396.

Gandhi S.M. and Sarkar B. C. (2016). Essentials of Mineral Exploration and Evaluation. Elsevier Science book. url:https://books.google.co.ke/books?id=WxChCgAAQBAJ.

Gunn, P., Maidment, D. and Milligan, P. 1997a. Interpreting aeromagnetic data in areas of limited outcrop. AGSO Journal of Australian Geology & Geophysics, 17(2), 175–185.

Hany, E. and Abdallah, I. A. E. (2014). Natural Radioactivity in Water samples from Assiut city, Egypt. International Journal of Pure and Applied Sciences and Technology, 22 (1), 44–52.

IAEA TECDOC 486 (2019). Guidelines on Soil and Vegetation Sampling for Radiological Monitoring. Vienna: International Atomic Energy Agency

ICRP (2000). Protection of the Public in Situations of Prolonged Radiation Exposure. ICRP Publication 82, Ann. ICRP, 29 (1-2), Oxford: Pergamon.

ICRP (2007). The 2007 Recommendations of the International Commission on Radiological Protection. ICRP Publication 103. Ann. ICRP 37 (2-4) Oxford: Pergamon.

Lu, X. W., & Zhang, X. L. (2006). Measurement of Natural Radioactivity in Sand Samples Collected from the Baoji Weihe Sands Park, China. Environmental Geology, 50, 977-982. https://doi.org/10.1007/s00254-006-0266-5

Monika, S., Leszek, P., & Marcin, Z. (2010). Natural Radioactivity of Soil and Sediment Samples Collected from Postindustrial Area, Poland. Polish Journal of Environmental Studies, 19, 1095-1099.

Nettleton, L.L. 1976. Gravity and Magnetics in oil prospecting. McGraw- Hill, New York, pp. 394-413.

Okpoli, C.C. and Akingboye, A.S. 2016. Magnetic, Radiometric and Geochemical Survey of Quarry Sites in Ondo State, Southwestern, Nigeria. International Basic and Applied Research Journal, Volume 2, Issue no. 8, pp. 16-30.

Otton, J. K. (1994). National Radioactivity in Environment. Retrieved February 2, 2019, from http://energy.usgs.gov/factsheets/radioactivity.

Report 108 (Rconnaisance) (1987). Ministry of Environment and Natural Resources, Mines and Geological department, Republic of Kenya.

Salem, A., Williams, S., Fairhead, J., Ravat, D. and Smith, R. 2007. Tilt-depth method: a simple depth estimation method using first-order magnetic derivatives. The Leading Edge, 26, 1502-1505.

ISSN 1561-7645 (online)
doi: 10.4314/jagst.v24i2.4

Taskin, H., Karavus, M., Ay, P., Topuzoglu, A., Hidiroglu, S., & Karahan, G. (2009). Radio-nuclide Concentrations in Soil and Lifetime Cancer Risk Due to Gamma Radioactivity in Kirklareli, Turkey. Journal of Environmental Radioactivity, 100, 49-53. https://doi.org/10.1016/j.jenvrad.2008.10.012

Telford, W.M., Geldart, L.P. and Sheriff, R.E. 1990. Applied Geophysics (Second edition). Cambridge University Press.

Tzortzis, M. and Tsertos, H. (2004). Determination of thorium, uranium and potassium elemental cocentrations in surface soils in Cyprus. Journal of environmental radioactivity, 77 (3), 325–338.

UNSCEAR (2000). Sources and Effects of Ionizing Radiation. United Nation Scientific Committee on the Effects of Atomic Radiation Sources to the General Assembly with Annexes, Effects and Risks of Ionizing Radiation, New York: United Nations Publication.

UNSCEAR (2008). Sources and Effects of Ionizing Radiation. United Nation Scientific Committee on the Effects of Atomic Radiation Sources to the General Assembly with Annexes, Report to the General Assembly, with Scientific Annexes, New York: United Nations Publication.

Wafula, C., Njogu, P., Kikuvi, G. ., Kamau, J. N., & Mburu, C. (2022). Occupational Exposure to Radiation in Open cast Artisanal and Small-Scale Gold Mining in Western Kenya. *JOURNAL OF AGRICULTURE, SCIENCE AND TECHNOLOGY*, *21*(3), 22–29. https://doi.org/10.4314/jagst.v21i3.3

WHO, World Health Organisation (2006). Guidelines for Drinking Water Quality: 3rd edition. Chapter 9; Radiological aspects. At http://www.who.int/water_sanitation_health/dwq/gdwq3rev/en/index.

WHO, World Health Organisation (2008). Guidelines for Drinking Water Quality, 3rd edition in cooperating the 1st Agenda vol. 1 Recommendations; Radiological aspect Geneva: WHO Geneva.

ISSN 1561-7645 (online)
doi: 10.4314/jagst.v24i2.4